ORAL/POSTER REFERENCE: ICF100832OR

ANALYSIS OF THREE-DIMENSIONAL INTERFACE CRACKING IN ELECTRONIC PACKAGES

A. O. Ayhan and H. F. Nied

Department of Mechanical Engineering
and Applied Mechanics, Lehigh University
Bethlehem, PA 18015-3085, USA

ABSTRACT

A technique for calculation of stress intensity factors for three-dimensional interface surface crack problems is presented. Of special interest, is the analysis of interface delamination observed in electronic packaging subjected to thermal cycling. Using a finite element approach, enriched 3-D interface crack tip elements are developed for direct computation of stress intensity factors along the crack front. The enriched 3-D crack tip elements contain the asymptotic displacement and strain fields for interface cracks. For cracks located between silicon and polymeric underfill materials in electronic packaging, the mode I and mode II stress intensity factors can be strongly coupled, since these materials yield relatively large values for Dunders' parameters. It is demonstrated that the enriched interface crack tip element approach is a very efficient technique for obtaining stress intensity factors and strain energy release rates for general three-dimensional interface crack problems. Of particular interest in this study are the stress intensity factors for semi-circular and quarter-circular surface cracks on the interface between silicon and epoxy. The enriched element approach is particularly effective for obtaining mode I, II and III stress intensity factors in the small zone near the free surface where the strength of the stress singularity is known to change.

KEYWORDS

Interface Cracks, Electronic Packages, Finite Element Method, 3-D Surface Cracks.

INTRODUCTION

One of the most important failure mechanisms that needs to be considered in the design of electronic packages, is interfacial cracking between the various layers of dissimilar electronic materials, e.g., silicon and epoxy. Such cracking can arise due to thermal cycling and/or moisture diffusion into the electronic package. Large differences in coefficients of thermal and hygroscopic expansion provide the driving forces necessary for interfacial cracking between material layers with inherently weak interfacial adhesion. Typically, such cracking originates at edges and corners where high stress concentrations are known to exist. The most severe stress concentrations tend to occur at three-dimensional corners [1], leading to the type of three-dimensional corner cracking shown in Figure 1. This figure depicts crack growth due to

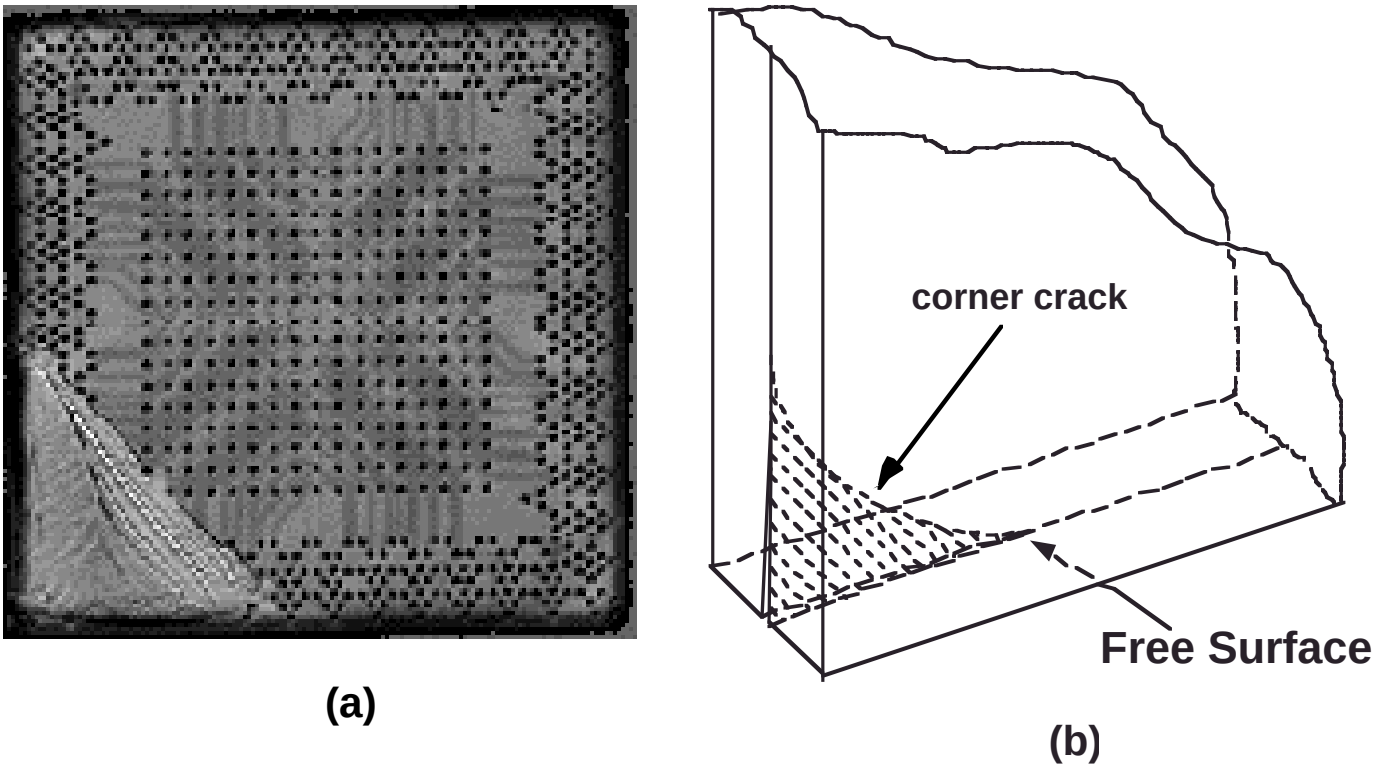

Figure 1: Interface cracking between silicon die and epoxy underfill in flip chip package. Crack emanating from corner after 300 cycles (-45°C - 125°C). Acoustic C-SAM image courtesy of David Peterson, Sandia National Laboratories.

thermal cycling between -45°C and +125°C. Crack growth under these conditions is inherently mixed-mode in nature with large mode II/III components. Application of interface fracture mechanics to predict debonding between layered materials has been extensively investigated and can serve as a basis for structural design for damage tolerance. This approach requires the accurate computation of stress intensity factors, K_I, K_{II}, and K_{III}, as well as strain energy release rates, G, for complex geometries and loading. The finite element method, suitably modified, can be used to compute these quantities for the complex interface cracking problems encountered in semiconductor packaging. A particularly effective approach is the use of "enriched" 3-D interface crack tip elements for direct computation of stress intensity factors [2]. The enriched crack tip elements contain the closed-form asymptotic solutions for displacements and strains in addition to the usual polynomial interpolation functions. Following this approach, the stress intensity factors are additional degrees of freedom computed directly in the same manner as the nodal displacements. One advantage of this approach is that there is no need for a special crack tip mesh, e.g., refined "tunnel" mesh or relocation of nodes to obtain a suitable singular solution. As long as the enriched elements are properly integrated and transition elements are used to maintain displacement compatibility, automatically generated meshes are adequate for highly accurate results.

FINITE ELEMENT FORMULATION

Enriched Crack Tip Elements

The enriched finite element formulation for interface crack problems is an extension of concepts introduced by Benzley [3] for conventional isotropic fracture problems. Application of the enrichment technique to interfacial fracture problems is relatively straightforward for two-dimensional problems once the asymptotic crack tip displacement and strain fields have been derived. In [4], an enriched crack tip element for interface cracks between dissimilar isotropic media is developed. Reference [5] documents a similar formulation for modeling interface cracks between orthotropic materials.

We have developed 3-D enriched elements for a variety of elements with various polynomial shape functions. For example, Figure 2a depicts a 32-noded enriched hexahedron element that uses cubic polynomial interpolation functions for displacements. In addition to the 96 displacement degrees of freedom

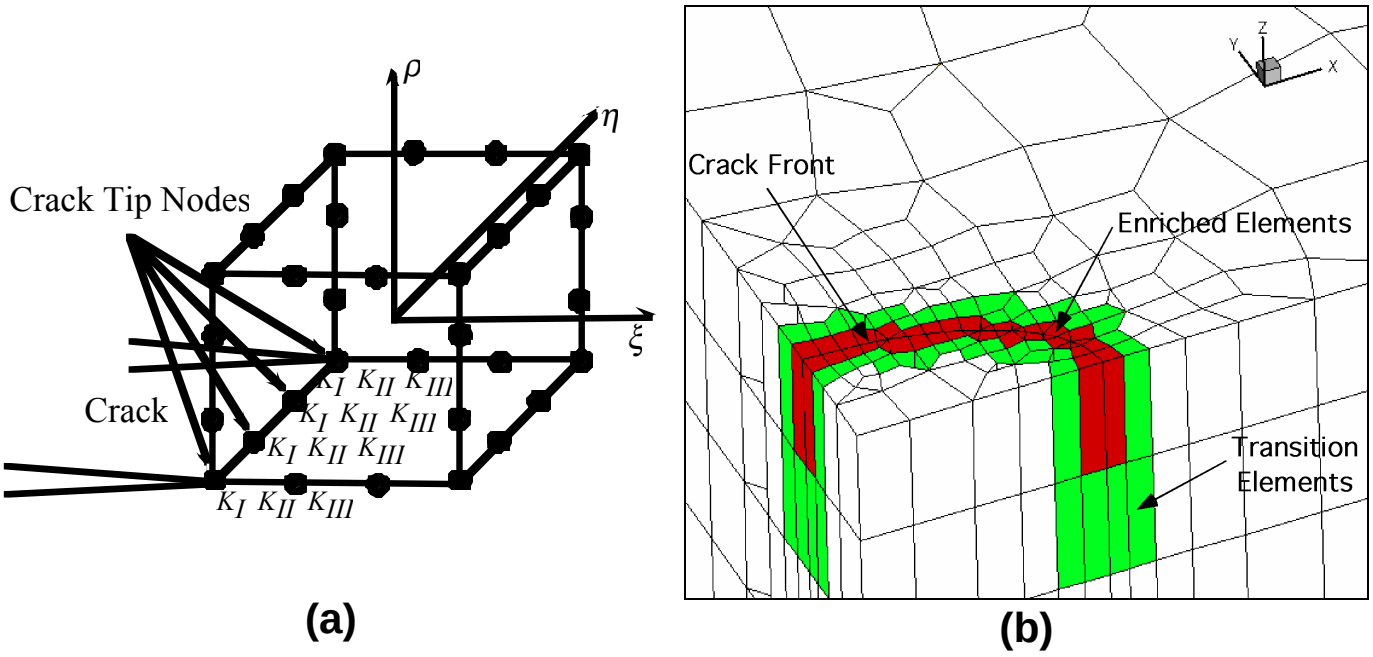

Figure 2: a) Enriched cubic hexahedron showing crack tip nodes. b) Semi-elliptic surface crack showing location of enriched crack tip elements and adjacent transition elements.

this element also has 12 unknowns representing the stress intensity factors K_I, K_{II}, and K_{III}, at nodes on the crack front. Thus, for this particular element there are 108 unknowns. Since the enriched crack tip element contains non-polynomial analytic terms, displacement compatibility cannot be ensured with neighboring elements that do not contain the asymptotic terms. To enforce displacement compatibility between all elements, transition elements should be used between the fully enriched crack tip elements and the regular elements. The location of these transition elements is shown in Figure 2b. Transition elements also contain the asymptotic fields for displacements and strains, but this contribution to the element stiffness matrix is linearly zeroed out across the volume of the element. The relevant details for 3-D transition elements are given by Ayhan in [6]. The components of displacement field for enriched 3-D elements of the type shown in Figure 2 are given by

$$u(\xi,\eta,\rho)=\sum_{j=1}^{nodel}N_j(\xi,\eta,\rho)u_j+Z_0(\xi,\eta,\rho)\sum_{i=1}^{ntip}N_i(\bar{\xi})K_I^i\left(f_1(\xi,\eta,\rho)-\sum_{j=1}^{nodel}N_j(\xi,\eta,\rho)f_{1j}\right)$$
$$+Z_0(\xi,\eta,\rho)\sum_{i=1}^{ntip}N_i(\bar{\xi})K_{II}^i\left(g_1(\xi,\eta,\rho)-\sum_{j=1}^{nodel}N_j(\xi,\eta,\rho)g_{1j}\right) \quad (1)$$

$$v(\xi,\eta,\rho)=\sum_{j=1}^{nodel}N_j(\xi,\eta,\rho)v_j+Z_0(\xi,\eta,\rho)\sum_{i=1}^{ntip}N_i(\bar{\xi})K_I^i\left(f_2(\xi,\eta,\rho)-\sum_{j=1}^{nodel}N_j(\xi,\eta,\rho)f_{2j}\right)$$
$$+Z_0(\xi,\eta,\rho)\sum_{i=1}^{ntip}N_i(\bar{\xi})K_{II}^i\left(g_2(\xi,\eta,\rho)-\sum_{j=1}^{nodel}N_j(\xi,\eta,\rho)g_{2j}\right) \quad (2)$$

$$w(\xi,\eta,\rho)=\sum_{j=1}^{nodel}N_j(\xi,\eta,\rho)w_j+Z_0(\xi,\eta,\rho)\sum_{i=1}^{ntip}N_i(\bar{\xi})K_{III}^i\left(h(\xi,\eta,\rho)-\sum_{j=1}^{nodel}N_j(\xi,\eta,\rho)h_j\right). \quad (3)$$

The first summation terms in (1)-(3) represent the usual displacements in regular isoparametric elements, i.e., N_i are the interpolation functions in element coordinates (ξ,η,ρ) and u_i,v_i,w_i, are the nodal displacements. Z_0. is the "zeroing function" that provides inter-element compatibility between the crack tip elements and the elements that surround the enriched elements. In a typical transition element, Z_0=1 at the nodal points where the transition element is adjacent to any of the crack tip elements, and is 0 when adjacent

to regular isoparametric elements. K^i_I , K^i_{II} , and K^i_{III} 's are the unknown stress intensity factors, for modes I, II, and III, respectively. For the cubic element, with four crack tip nodes, K^i_I , K^i_{II} , and $K^i_{I,}$ are interpolated using the cubic polynomial shape function associated with the displacements at these same nodes. The functions f_1, f_2, g_1, g_2, and h are the asymptotic displacement terms that are coefficients of the mode I, II and III stress intensity factors [3-5]. The terms f_{1j} , f_{2j} , g_{1j} , g_{2j} , and h_j are the asymptotic crack tip displacement expressions evaluated at the jth node in the element. It is well known that the asymptotic crack tip fields in three dimensions are identical to two-dimensional fields in plane strain, with the possible exception of points where the three-dimensional crack front terminates on a free surface. For three-dimensional analysis, the plane strain crack tip fields are evaluated in planes that are perpendicular to the crack front. Thus, during integration to calculate the element stiffness matrix, the perpendicular distance to the crack front r, as well as the angular orientation θ, with respect to the plane of the crack, must be determined for evaluation of the asymptotic displacements and strains. Since the element stiffness matrix is determined with respect to a global coordinate system, the asymptotic expressions computed in the local crack tip coordinate system must be transformed back to global coordinates.

Crack Tip Fields for Interface Cracks

The elastic singular stress field near the tip of an interface crack differs from that of a crack in a homogeneous material and exhibits an oscillatory behavior near the crack tip region. The singular stress field for a three-dimensional interface crack is given by

$$\sigma_{ij} = \frac{1}{\sqrt{2\pi r}}\left\{\mathrm{Re}\left[\mathrm{K}r^{i\varepsilon}\right]\tilde{\sigma}^{I}_{ij}(\theta,\varepsilon) + \mathrm{Im}\left[\mathrm{K}r^{i\varepsilon}\right]\tilde{\sigma}^{II}_{ij}(\theta,\varepsilon) + K_{III}\tilde{\sigma}^{III}_{ij}(\theta)\right\} \tag{4}$$

where r and θ are the polar coordinates in the local coordinate system that is located on the crack front in planes perpendicular to the crack front. The complex stress intensity factor **K** is defined by K_I+iK_{II} and $\tilde{\sigma}_{ij}$'s are the angular stress variation terms for different modes of loading. The complex singularity in (4) depends on the oscillatory index, ε, given by

$$\varepsilon = \frac{1}{2\pi}\ln\left[\frac{1-\beta}{1+\beta}\right] \ . \tag{5}$$

In (5) β is the second Dunders' parameter. Dunders' parameters for bimaterial problems are defined by

$$\alpha = \frac{\mu_1(\kappa_2+1)-\mu_2(\kappa_1+1)}{\mu_2(\kappa_1+1)+\mu_1(\kappa_2+1)}, \quad \beta = \frac{\mu_1(\kappa_2-1)-\mu_2(\kappa_1-1)}{\mu_2(\kappa_1+1)+\mu_1(\kappa_2+1)} \ , \tag{6}$$

with μ the shear modulus and κ=3-4ν for plane strain (ν is Poisson's ratio). The subscripts for μ, κ and ν in (6) identify the different materials on either side of the interface. For the silicon/epoxy materials used in this study, the oscillatory index ε=0.066 and Dunders' parameters are given by α = -0.8235, β=-0.2044.

RESULTS

In an effort to investigate interfacial crack solutions for three-dimensional (curved) crack fronts on silicon/epoxy interfaces, two different crack geometries are presented: 1) A semi-circular surface crack (Fig. 3a) and 2) A quarter-circular corner crack (Fig. 3b). Solutions are given for uniform tensile loading and thermal loading. A typical finite element model had 3400 elements consisting of 32-noded cubic hexahedrons and 26-node cubic pentahedrons with 26984 nodes. Because of the oscillatory form of the mode I and mode II interface stress intensity factors (4), the presented stress intensity factors are "rotated" using a procedure described by Rice [6], i.e.,

$$K^R_j = K_j L^{i\varepsilon} \ , \qquad j = 1,2 \tag{7}$$

$$K^R_{III} = K_{III} \ . \tag{8}$$

In (7) L is a constant arbitrarily set as 2 meters. In addition, the plotted results are normalized using the solution for a penny shaped crack, i.e., $K_{IR} = \frac{2}{\pi}\sigma_0(\pi a)^{1/2}$.

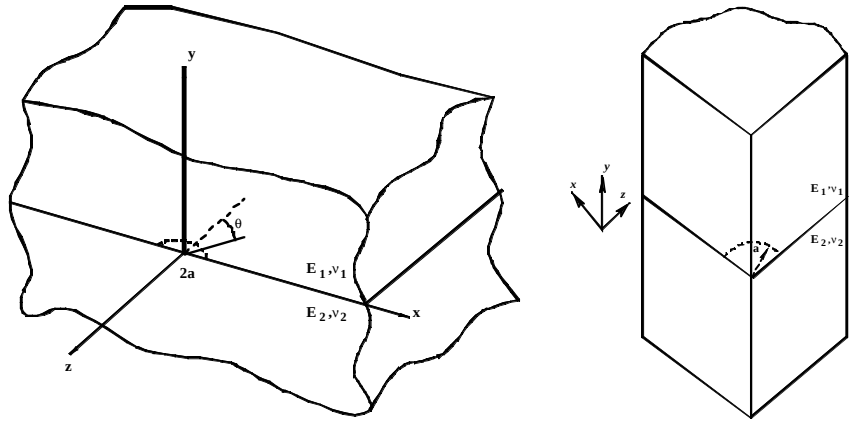

Figure 3: a) Semi-circular surface crack b) Quarter-circular corner crack.

Interfacial Surface and Corner Cracks Subjected to Uniform Tension

Figure 4a shows the normalized rotated stress intensity factors along the crack front for the case of a semi-circular surface crack on the interface between silicon and epoxy loaded in uniaxial tension. The results are given as a function of the angle θ measured from the plane of symmetry. Note that the mode I stress intensity factor increases significantly as the free surface is approached and in the neighborhood of this surface is 50% greater than the mode I stress intensity factor in the interior. K_{II}, on the other hand, decreases from the symmetry plane towards the free surface and K_{III} increases in magnitude having a negative sign. For the quarter-circular corner crack (Figs. 3b & 4b), the results are symmetric with respect to the θ=45^o plane. We also note that, although K_{II} remains almost constant along the front, a higher mode I stress intensity factor is seen near θ=45^o (middle region) than it was near the mid-plane (θ=0) for the interfacial semi-circular surface crack problem. In both problems, the mode III component of the stress intensity factor also takes its maximum value near the free surface region.

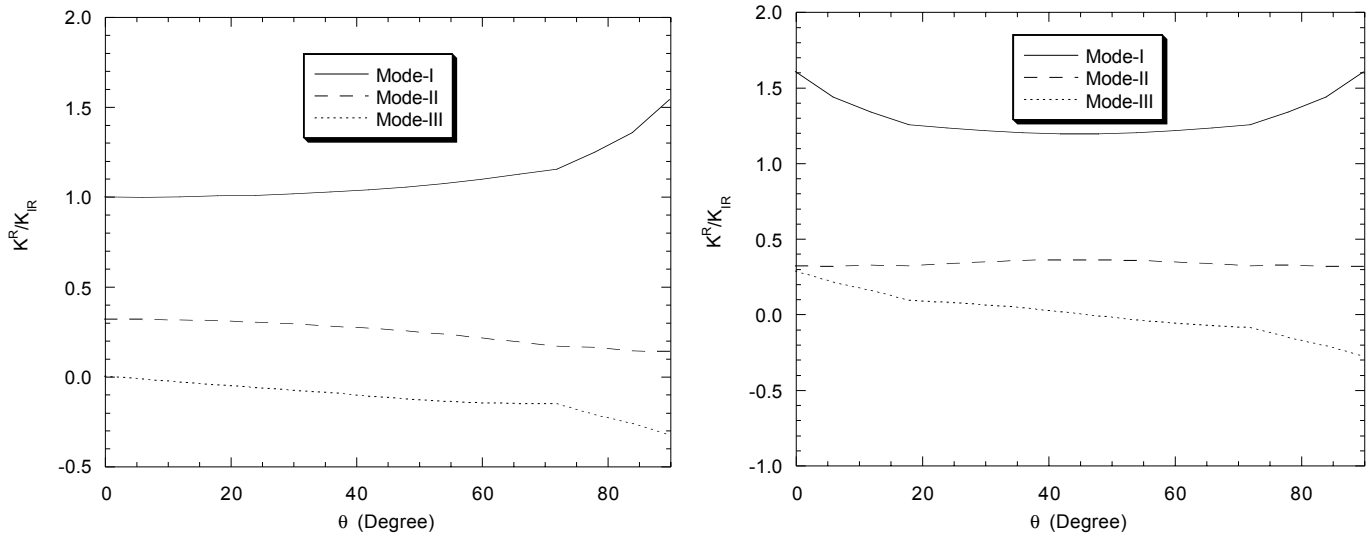

Figure 4: Normalized stress intensity factors for silicon-epoxy interface cracks subjected to uniform tensile loading. a) Semi-circular surface crack. b) Quarter-circular corner crack.

Interfacial Surface and Corner Cracks Subjected to Thermal Loading

Fig. 5a depicts the stress intensity factors along the crack front for the case of interfacial semi-circular surface crack subjected to -1^{o}C uniform cooling. There are no boundary restraints in either of these models. Normalization is again with respect to the penny shaped crack mode I solution with $\sigma_0 = 1$. As in the preceding case, K_I and K_{III} see a substantial increase as the free surface is approached. The other important point is that for thermal loading problems, the mode II and mode III stress intensity factors become as

important as the mode I component. This reflects the high mode mixity that occurs for this type of loading. It can be seen in the figures that K_{II} takes its maximum value on the symmetry plane (θ=0^o) whereas K_{III} becomes maximum in magnitude on the free surfaces. Note also that near the symmetry plane, K_I is negative. For a homogeneous crack problem this would indicate that the crack surfaces are in large-scale contact, but it is not so in this case. Because of the definition of the stress intensity factor in the bimaterial case, having a negative K_I does not always mean large scale crack surface contact, as it would in the homogeneous case. Of course, the asymptotic crack tip contact associated with the oscillatory crack tip behavior is present, but this is another matter. The stress intensity factors shown in Fig. 5b are for the case of a quarter-circular corner crack on the silicon-epoxy interface with a -1^{o}C uniform temperature change. Again, the results are symmetric with respect to θ=45^o plane and K_I and K_{II} have their maximum values near the free surface whereas K_{II} has a maximum value at θ=45^o. Comparing the results with the previous surface crack solution (Fig. 4), it can be seen that near the free surface region, the order of magnification in K_I and K_{III} are almost the same for both cases.

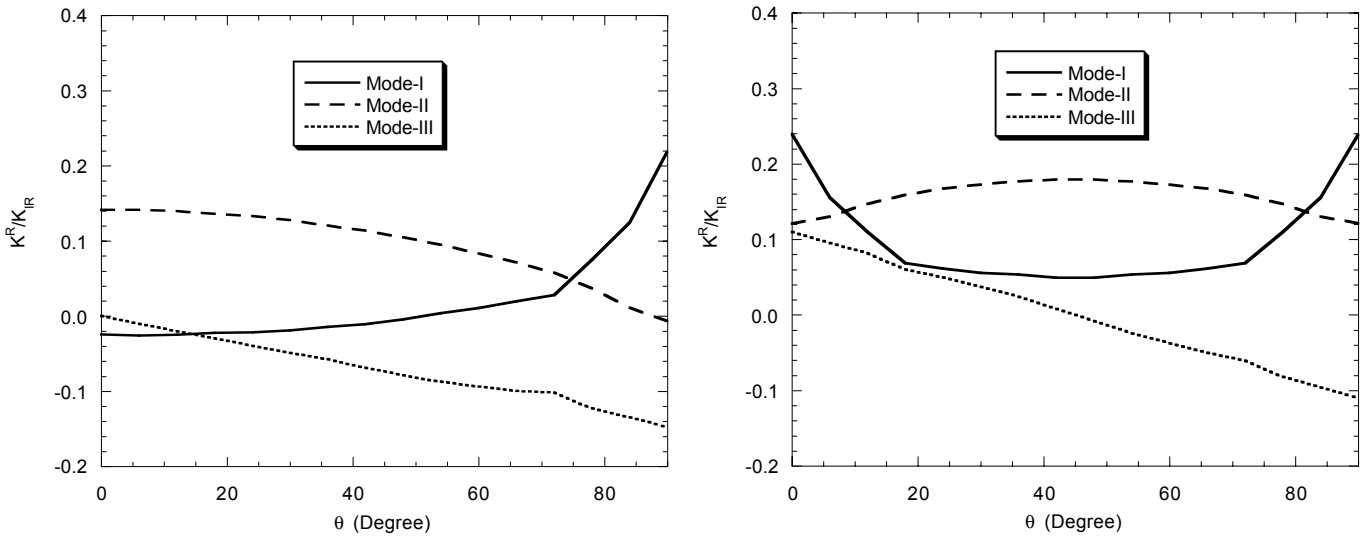

Figure 5: Normalized stress intensity factors for silicon-epoxy interface cracks subjected to -1^{o}C uniform cooling loading. a) Semi-circular surface crack. b) Quarter-circular corner crack.

ACKNOWLEDGEMENT

The support of the Semiconductor Research Corporation under Contract SRC 826.002 and a grant from General Electric's Corporate Research and Development Center is gratefully acknowledged.

REFERENCES

1. Xu, A. Q., and Nied, H. F., (2000), "Finite Element Analysis of Stress Singularities in Attached Flip Chip Packages," *ASME Journal of Electronic Packaging*, Vol. 122, pp. 301 - 305.
2. Ayhan, A. O., and Nied, H. F., (1999), "Finite Element Analysis of Interface Cracking in Semiconductor Packages," *IEEE Transactions on Components and Packaging Technology*, Vol. 22, No. 4, pp. 503 – 511.
3. Benzley, S. E., (1974) "Representation of Singularities with Isoparametric Finite Elements," *Int. J. Numer. Meth. Eng.*, vol. 8, pp. 537-545.
4. Chen, E. P., (1985) "Finite Element Analysis of a Bimaterial Interface Crack," *Theoretical Appl. Fracture Mech.*, vol. 3, pp. 257-262.
5. A. C. Kaya and H. F. Nied, (1993) "Interface Fracture Analysis of Bonded Ceramic Layers Using Enriched Finite Elements," *Ceramic Coatings*, MD-Vol. 44, edited by K. Kokini, Proceedings of the 1993 ASME Winter Annual Meeting, pp. 47-71.
6. Ayhan, A. O., "Finite Element Analysis of Nonlinear Deformation Mechanisms in Semiconductor Packages," (1999), Ph.D. Dissertation, Lehigh University.
7. Rice, J. R., "Elastic Fracture Mechanics Concepts for Interfacial Cracks," (1988), *J. of Appl. Mech.*, vol. 55, pp 98-103.